EXCLUSIVE $\rho\rho$ PRODUCTION IN $\gamma\gamma$ INTERACTION AT LEP*

I. Vorobiev†

(on behalf of the L3 Collaboration)

Carnegie Mellon University, Pittsburgh, PA 15213, USA

(Received January 2, 2006)

Exclusive $\rho\rho$ production in two-photon collisions is studied at LEP for quasi-real photons ($\gamma\gamma$, centre-of-mass energies $161\,\mathrm{GeV} \leq \sqrt{s} \leq 209\,\mathrm{GeV}$, total integrated luminosity $L = 698\,\mathrm{pb}^{-1}$) and one virtual photon ($\gamma\gamma^*$, $89\,\mathrm{GeV} \leq \sqrt{s} \leq 209\,\mathrm{GeV}$ $L = 855\,\mathrm{pb}^{-1}$). The cross sections of the $\rho\rho$ production processes are determined as a function of the photon virtuality, Q^2, and the two-photon centre-of-mass energy, $W_{\gamma\gamma}$, in the kinematic region: $Q^2 \leq 30\,\mathrm{GeV}^2$ and $1\,\mathrm{GeV} \leq W_{\gamma\gamma} \leq 3\,\mathrm{GeV}$.

PACS numbers: 13.60.Le

1. Introduction

Measurements of exclusive $\rho\rho$ production in $\gamma\gamma$ interactions have been performed previously mainly for quasi-real photons (see, for example [1]) with Q^2 close to zero, while only scarce data on higher Q^2 production exist (for example [2]).

Recently a QCD model was proposed [3] for calculating the cross section of exclusive meson pair production in gamma–gamma interactions with one highly virtual photon having $Q^2 \gg W_{\gamma\gamma}$. In this model the exclusive process is factorisable into a perturbative, calculable, short distance scattering $\gamma\gamma^* \to q\bar{q}$ or $\gamma\gamma^* \to gg$ and non-perturbative matrix elements, which are called generalized distribution amplitudes, describing the transition of the two partons into hadron pairs.

The L3 Collaboration performed a series of measurements of neutral and charged ρ-meson pair production in interactions with two quasi-real photons

$$e^+e^- \to e^+e^-\gamma\gamma \to e^+e^-\rho\rho\,, \tag{1}$$

* Presented at the PHOTON2005 Conference, 31 August–4 September 2005, Warsaw, Poland.

† Present address: CERN, 1211 Geneva 23, Switzerland; `Igor.Vorobiev@cern.ch`

and with one photon of higher virtuality

$$e^+e^- \to e^\pm e^\mp{}_{\mathrm{tag}}\gamma\gamma^* \to e^\pm e^\mp{}_{\mathrm{tag}}\rho\rho\,. \tag{2}$$

In reaction (1) both electron and positron escape detection (untagged events), while in reaction (2) one electron/positron is tagged either by the Luminosity Monitor (LUMI) or Very Small Angle Tagger (VSAT) ($\rho^0\rho^0$ with the LUMI, Ref. [4], $\rho^+\rho^-$ with the LUMI, Ref. [5], $\rho^0\rho^0$ with the VSAT, Ref. [6], $\rho^+\rho^-$ with the VSAT, Ref. [7], paper for untagged measurements is in preparation). The LUMI covers the Q^2 range 1.2–8.5 GeV^2 at LEPI, 8.8–30 GeV^2 at LEPII, and the VSAT (available only at LEPII) 0.2–0.85 GeV^2.

2. Measurements

Untagged measurements were done at LEPII (161 GeV $\leq \sqrt{s} \leq$ 209 GeV) with an integrated luminosity $L = 697.7\,\mathrm{pb}^{-1}$. Measurements with the LUMI — at LEPI ($\sqrt{s}$ around 91 GeV) with $L = 148.7\,\mathrm{pb}^{-1}$ and at LEPII (161 GeV $\leq \sqrt{s} \leq$ 209 GeV) with $L = 706.0\,\mathrm{pb}^{-1}$, measurements with the VSAT — at LEPII (183 GeV $\leq \sqrt{s} \leq$ 209 GeV) with $L = 684.8\,\mathrm{pb}^{-1}$. The underlying selected reactions are:

$$e^+e^- \to e^+e^-\pi^+\pi^-\pi^+\pi^-\,, \tag{3}$$
$$e^+e^- \to e^+e^-\pi^+\pi^-\pi^0\pi^0\,, \tag{4}$$
$$e^+e^- \to e^\pm e^\mp{}_{\mathrm{tag}}\pi^+\pi^-\pi^+\pi^-\,, \tag{5}$$
$$e^+e^- \to e^\pm e^\mp{}_{\mathrm{tag}}\pi^+\pi^-\pi^0\pi^0\,. \tag{6}$$

For reaction (3) 74859 events were selected, and for reaction (4) 7535 events. 934 events of reaction (5) were selected in the LUMI sample and 1938 in the VSAT one. For reaction (6) 343 and 414 events, respectively. An example of the distributions for selected events (for reaction (6) with the VSAT) is shown in Fig. 1. The mass distribution of charged pion pairs (Fig. 1(b)) shows a strong signal of $\rho^\pm$ production, and the two-dimensional distribution of such masses (Fig. 1(c)) presents a concentration of events in the region of a $\rho^+\rho^-$ signal. No structure is observed in the correlation plot of $\pi^+\pi^-$ and $\pi^0\pi^0$ mass combinations (Fig. 1(d)), as expected. For further analysis and cross section determination the events in the region 1.1 GeV $\leq W_{\gamma\gamma} \leq$ 3 GeV were kept (Fig. 1(a)).

For untagged events (reactions (3), (4)) a spin-parity-helicity analysis was employed according to the model used in [1]. The $\rho\rho$ production was considered in different spin-parity and helicity states (J^P, J_Z) together with an isotropic nonresonant production of four pions. It was checked that the inclusion of the $\rho\pi\pi$ state practically did not change the results on $\rho\rho$ production.

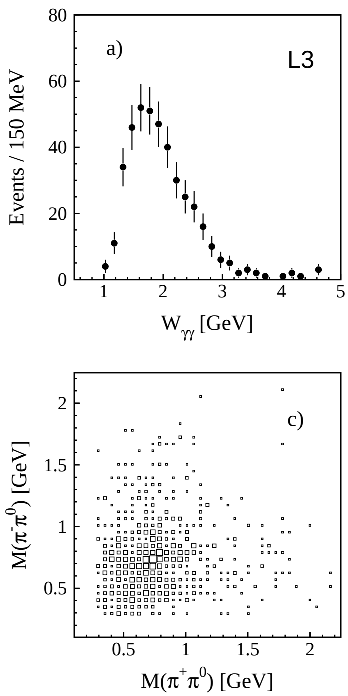

Fig. 1. Mass distributions for the selected $\pi^+\pi^-\pi^0\pi^0$ events with VSAT tag: (a) the four-pion system mass, $W_{\gamma\gamma}$; (b) the $\pi^\pm\pi^0$ combinations (four entries per event); (c) correlation between the $\pi^-\pi^0$ and $\pi^+\pi^0$ pairs (two entries per event) and (d) correlation between the $\pi^+\pi^-$ and $\pi^0\pi^0$ pairs.

In order to determine the differential $\rho\rho$ production rates in tagged events (reactions (5), (6)), a maximum likelihood fit was performed in intervals of Q^2 and $W_{\gamma\gamma}$ using a box method. Data were fit to the sum of non-interfering contributions from the processes, generated by a Monte Carlo in a simple model of isotropic production and phase space decay. For the data sample with the LUMI the processes used in fit were: for the reaction (5): $\gamma\gamma^* \to \rho^0\rho^0$, $\gamma\gamma^* \to \rho^0\pi^+\pi^-$, $\gamma\gamma^* \to \pi^+\pi^-\pi^+\pi^-$ (nonresonant); for the reaction (6): $\gamma\gamma^* \to \rho^+\rho^-$, $\gamma\gamma^* \to \rho^\pm\pi^0\pi^0$, $\gamma\gamma^* \to \pi^+\pi^-\pi^0\pi^0$ (nonresonant). For the data sample with the VSAT it was found that the fit is improved if we include additional channels — for the reaction (5): $\gamma\gamma^* \to f_2(1270)\pi^+\pi^-$ and for the reaction (6): $\gamma\gamma^* \to a^\pm{}_2(1320)\pi^0$ (we do not determine the cross sections of these processes). The inputs to the fit were the six possible two-pion mass combinations in an event. The fit provides a good description of all mass and angular distributions. From the numbers of $\rho\rho$ events, obtained by the fit in intervals of Q^2 and $W_{\gamma\gamma}$ and corrected for efficiencies and background, the cross sections of $\rho\rho$ pair production were calculated.

3. Results

The measured cross sections in untagged events for different $\rho\rho$ states and the 4π contribution are shown on Fig. 2. The results confirm previous observations [1] with higher statistical precision: the dominant $\rho\rho$ contribution is in the state $(2^+, 2)$, below a mass of about 2 GeV $\rho^0\rho^0$ cross section is few times higher than the $\rho^+\rho^-$ one.

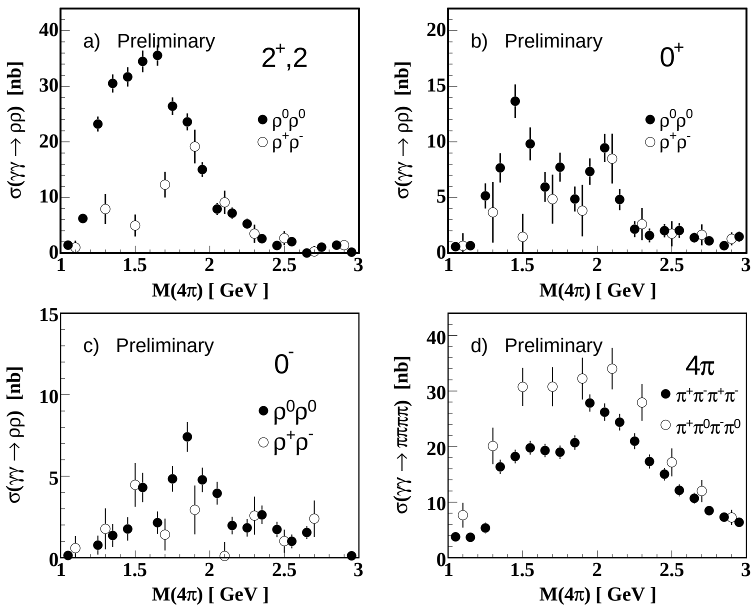

Fig. 2. Measured $\gamma\gamma \to \rho^0\rho^0$ and $\gamma\gamma \to \rho^+\rho^-$ cross sections for the states (a) $(2^+, 2)$, (b) 0^+, (c) 0^- and (d) for nonresonant contribution $\gamma\gamma \to 4\pi$.

The cross section dependences on Q^2 and $W_{\gamma\gamma}$ for both $\rho^0\rho^0$ and $\rho^+\rho^-$ production are shown in Figs. 3 and 4. The Q^2 dependence of the differential cross section can be well described by the approximate formula

$$\frac{d\sigma_{ee}}{dQ^2} \sim \frac{1}{Q^n}\Big(Q^2 + \langle W_{\gamma\gamma}\rangle^2\Big)^2, \tag{7}$$

following QCD-based calculations [8], where n is expected to equal 2. In the range $Q^2 > 1.2$ GeV^2, the fit gives values $n = 2.4 \pm 0.3$ for $\rho^0\rho^0$ and $n = 2.5 \pm 0.4$ for $\rho^+\rho^-$, which are compatible with the expected value of 2. The $\rho^0\rho^0$ production at $Q^2 > 1.2$ GeV^2 was analyzed in paper [9]. The Q^2 dependence of the differential cross section is perfectly reproduced by the formulas with three phenomenological parameters, one of which, $C_1 = 1.20 \pm 0.23$ GeV^2, gives the normalization of the $\rho\rho$ generalized distribution amplitudes. In the $Q^2 > 0.2$ GeV^2 range, the fit to approximate formula (7) gives $n = 2.3 \pm 0.15$ for $\rho^+\rho^-$ and $n = 2.9 \pm 0.14$ for $\rho^0\rho^0$ (fit is shown in Fig. 3(a) by the lines).

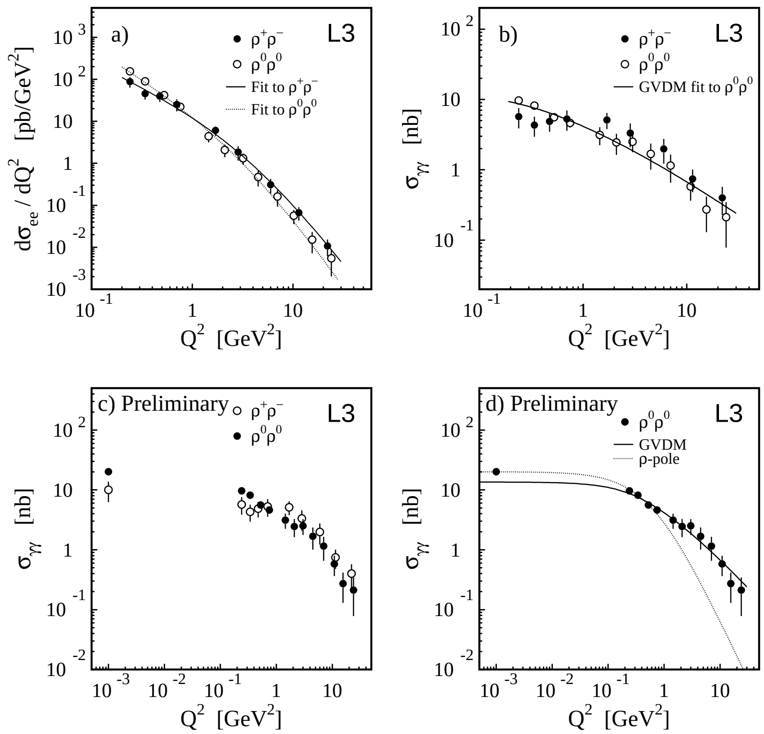

Fig. 3. The $\rho\rho$ production cross section as a function of Q^2: (a) differential cross section of the process $e^+e^- \to e^\pm e^\mp{}_{\mathrm{tag}}\rho\rho$, (b) cross section of the process $\gamma\gamma^* \to \rho\rho$, (c) $\sigma_{\gamma\gamma}$ cross section comparison for $\rho^+\rho^-$ and $\rho^0\rho^0$ for the whole range of Q^2, (d) $\sigma_{\gamma\gamma}$ for $\rho^0\rho^0$ with ρ-pole and GVDM fit.

The measured cross section of the process $\gamma\gamma^* \to \rho\rho$ as a function of Q^2 is shown in Fig. 3(b). It is well described by the GVDM model for $\rho^+\rho^-$ at $Q^2 > 1$ GeV^2 and for $\rho^0\rho^0$ in the entire Q^2 range. The fit for $\rho^0\rho^0$ in the whole Q^2 range finds a cross section of 13.6 ± 0.7 nb at $Q^2 = 0$ (Fig. 3(d)). A ρ-pole description is excluded for both $\rho^0\rho^0$ and $\rho^+\rho^-$ data.

The ratio of cross sections $R = \sigma_{e^+e^-\to e^+e^-\rho^+\rho^-}/\sigma_{e^+e^-\to e^+e^-\rho^0\rho^0}$ for 1.1 GeV $\leq W_{\gamma\gamma} \leq$ 2.1 GeV is $2.2 \pm 1.1 \pm 0.6$ in the Q^2 range 8.8 GeV$^2 \leq Q^2 \leq$ 30 GeV^2 (Fig. 4(d)) and $1.81 \pm 0.47 \pm 0.22$ for 1.2 GeV$^2 \leq Q^2 \leq 8.5$ GeV^2 (Fig. 4(c)). This is very compatible with the factor 2, expected for an isospin $I = 0$ state.

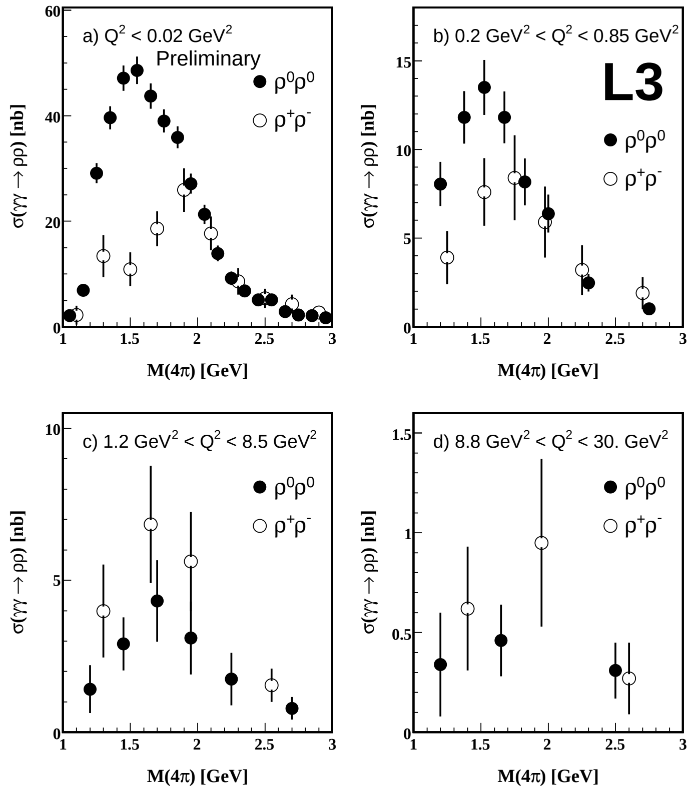

Fig. 4. The $\rho\rho$ production cross section as a function of $W_{\gamma\gamma}$ in four Q^2 intervals.

Contrary to this the measurements at lower Q^2 show the $\rho^0\rho^0$ cross section to be higher than the $\rho^+\rho^-$ one, $R = 0.63 \pm 0.10 \pm 0.09$ for 0.2 GeV^2 $\leq Q^2 \leq 0.85$ GeV^2 (Fig. 4(b)) and $0.42 \pm 0.05 \pm 0.09$ for $Q^2 \leq 0.02$ GeV^2 (Fig. 4(a)). The change of the relative magnitude of $\rho^+\rho^-$ and $\rho^0\rho^0$ production in the vicinity of $Q^2 \approx 1$ GeV^2 is clearly seen in Fig. 3(c), suggesting different ρ-pair production mechanisms at low and high Q^2.

If to assume the production of an isospin $I = 2$ exotic state at small Q^2, the whole ensemble of data can be well described for $Q^2 > 0.2$ GeV^2 (both Q^2 and $W_{\gamma\gamma}$ dependencies for $\rho^0\rho^0$ and $\rho^+\rho^-$, and change of relative amplitude in vicinity of $Q^2 \approx 1$ GeV^2) [10].

4. Conclusions

This is the first measurement of tagged exclusive $\rho^+\rho^-$ production in $\gamma\gamma$ interactions and more precise measurement of tagged $\rho^0\rho^0$ production. The untagged $\rho\rho$ measurement is performed with an order of magnitude higher statistics. The measurements allow us to follow the evolution of cross sections over a Q^2-range of four orders of magnitude. A QCD-based form is found to provide a good parametrization in the $Q^2 > 0.2$ GeV^2 interval, where the differential cross sections show a monotonic decrease of more than four orders of magnitude (for the $W_{\gamma\gamma}$ range 1.1 GeV $\leq W_{\gamma\gamma} \leq$ 3 GeV). The Q^2 dependence of the process $\gamma\gamma^* \to \rho^0\rho^0$ is well reproduced by a parametrization based on the GVDM model over the entire Q^2-region. But the $\rho^+\rho^-$ data cannot be satisfactory described by such a parametrization in the whole Q^2-region, only at $Q^2 > 1$ GeV^2. A ρ-pole description is excluded for both $\rho^0\rho^0$ and $\rho^+\rho^-$ data. The relative magnitude of $\rho^+\rho^-$ and $\rho^0\rho^0$ production changes in the vicinity of $Q^2 \approx 1$ GeV^2, suggesting different ρ-pair production mechanisms at low and high Q^2, in agreement with the hypothesis of an $I = 2$ exotic $\rho\rho$ state. These data lay new experimental grounds for obtaining information about QCD in going from nonperturbative to the perturbative regime.

REFERENCES

[1] TASSO Collab., M. Althoff *et al.*, *Z. Phys.* **C16**, 13 (982); ARGUS Collab., H. Albrecht *et al.*, *Z. Phys.* **C50**, 1 (1991); ARGUS Collab., H. Albrecht *et al.*, *Phys. Lett.* **B267**, 535 (1991).

[2] PLUTO Collab., Ch. Berger *et al.*, *Z. Phys.* **C38**, 521 (1988).

[3] M. Diehl *et al.*, *Phys. Rev. Lett.* **81**, 1782 (1998); N. Kivel, L. Mankiewicz, M.V. Polyakov, *Phys. Lett.* **B467**, 263 (1999); A. Freund, *Phys. Rev.* **D61**, 074010 (2000).

[4] L3 Coll., P. Achard *et al.*, *Phys. Lett.* **B568**, 11 (2003).

[5] L3 Coll., P. Achard *et al.*, *Phys. Lett.* **B597**, 26 (2004).

[6] L3 Coll., P. Achard *et al.*, *Phys. Lett.* **B604**, 48 (2004).

[7] L3 Coll., P. Achard *et al.*, *Phys. Lett.* **B615**, 19 (2005).

[8] M. Diehl, T. Gousset, B. Pire, *Phys. Rev.* **D62**, 073014 (2000).

[9] I.V. Anikin, B. Pire, O.V. Teryaev, *Phys. Rev.* **D69**, 014018 (2004).

[10] I.V. Anikin, B. Pire, O.V. Teryaev, `hep-ph/0506277`.